Targeting delivery of paclitaxel into tumor cells via somatostatin receptor endocytosis

Chun-Ming Huang*, Ying-Ta Wu* and Shui-Tein Chen

Background: The binding of somatostatin (SST) to endogenous G-protein-coupled receptors (SST receptors or SSTRs) is followed by internalization of SST, and, several reports have shown that a high density of SSTRs is present on most hormone-secreting tissue tumors. Facile synthesis of the long-acting SST analog, octreotide, has previously been described. Octreotide might be of practical value in developing tumor tracers and in serving as a carrier of cytotoxic antitumor drugs.

Results: Fluorescein-labeled octreotide was internalized into the cytosol of human breast MCF-7 carcinoma cells via binding to SSTRs. Octreotide-conjugated paclitaxel (taxol) was created by coupling taxol–succinate to the amino-terminal end of octreotide. This conjugate retains the biological activity of taxol in inducing formation of tubulin bundles, eventually causing apoptosis of MCF-7 cells. Cytotoxicity of octreotide-conjugated taxol is mainly mediated by SSTR, as shown by the observation that octreotide pretreatment can rescue the induced cell death. In comparison with free taxol, this conjugate shows much less toxicity in Chinese hamster ovary cells.

Conclusions: Octreotide-conjugated taxol exerts the same antitumor effect of free taxol on stabilizing microtubule formation and inducing cell death. This conjugate triggers tumor cell apoptosis mediated by SSTRs and is exclusively toxic to SSTR-expressing cells. Octreotide-conjugated taxol is less toxic to low-SSTR-expressing cells compared with free taxol. Our results strongly indicated that octreotide-conjugated taxol demonstrates cell selectivity and may be used as a targeting agent for cancer therapy.

Address: Institute of Biological Chemistry, Academia Sinica, Taipei 115, Taiwan.

Correspondence: Shui-Tein Chen
E-mail: bcchen@gate.sinica.edu.tw

*Contributed equally to this paper.

Key words: apoptosis, endocytosis, octreotide, paclitaxel, somatostatin

Received: **13 December 1999**
Revisions requested: **26 January 2000**
Revisions received: **7 March 2000**
Accepted: **17 March 2000**

Published: **9 June 2000**
Publication delayed at the author's request

Chemistry & Biology 2000, **7**:453–461

1074-5521/00/$ – see front matter

Introduction

Somatostatin (SST) is a neuropeptide that demonstrates a powerful inhibitory action against several endocrine systems. SST was originally isolated as an endocrine inhibitor of pituitary growth hormone secretion and is now recognized as a hormone capable of regulating fundamental processes, such as secretion, cell division, proliferation and apoptosis [1–3]. The cellular actions of SST are mediated by a family of GTP-binding-protein-coupled receptors, of which there are five (termed SSTR-1, -2, -3, -4 and -5) [4]. Most neuroendocrine tumors and their metastases express SSTRs to a much greater extent than do normal tissues [5–7]. The clinical usefulness of SST is limited, however, by its very short half-life. For therapeutic feasibility in humans, several synthetic SST analogs have been created with improved metabolic stability. A significant milestone in these efforts has been the design and synthesis of octreotide (SMS 201-995, Sandostatin^{TM}), an octapeptide analog of native SST [8]. This compound was found to be more potent than native SST in suppressing the release of growth hormone and to be more selective in its effects.

Since 1983, octreotide had been used therapeutically to prevent carcinoid crisis [9] and used also in clinical practice for the scintigraphic visualization of tumors containing a high density of SSTRs [10]. Lamberts *et al.* [11] and Krenning and co-workers [12] have demonstrated that radiolabeled octreotide derivatives ^{123}I–[Tyr^3]-octreotide and ^{111}In–diethylenetriamine penta-acetic acid (DTPA) octreotide are very useful for detecting small neuroendocrine tumors that cannot be detected by conventional means, and also for identifying tumors that respond to therapeutic doses of octreotide. Previously, we have described a facile synthesis of octreotide and its fluorescein-labeled derivative [13], which might serve as powerful tools for tumor identification. These promising results prompted us to develop octreotide as a specific carrier to deliver antitumor drugs, such as paclitaxel, into tumor cells via SSTR endocytosis.

Paclitaxel (or Taxol [Bristol-Myers Squibb, Princeton, NJ]) is a diterpenoid taxane derivative, which was first isolated from *Taxus brevifolia* by Wani *et al.* in 1971 (see [14] and references therein). It shows excellent antitumor activity in a wide variety of tumor models, such as B16 melanoma, L1210 and P388 leukemias, MX-1 mammary tumor and CX-1 colon tumor xenografts [15–17]. The antitumor property of taxol is due to its ability to promote tubulin assembly

into microtubules [18]. In the presence of taxol, microtubules resist depolymerization, thus interfering with the G_2 and M phases of the cell cycle [19]. In spite of its excellent antitumor activity, there are considerable difficulties in developing taxol as a chemotherapeutic agent — one major difficulty is that taxol is not cell specific.

In the present study, fluorescein-labeled octreotide is synthesized and used to verify specific receptor binding activities. It was used also to trace the intracellular localization of such activities. Simultaneously, we describe the synthesis of taxol linked to octreotide by chemical conjugation. Using MCF-7 and CHO cells as models, a comparison of cytotoxicity and cell specificity between taxol and octreotide-conjugated taxol was made. Our aim was to evaluate the role of octreotide-conjugated taxol in SSTR-mediated internalization and in tubulin binding followed by programmed cell death, in low- and high-density SSTR-expressing cells.

Results and discussion

Effects of octreotide on cell viability of MCF-7 cells

MCF-7 human breast cancer cells were cultured in Dulbecco's modified Eagle's medium (DMEM) containing 1% bovine fetal serum in the absence or the presence of the SST analog octreotide for one to seven days. Treatment of octreotide for up to three days did not significantly alter the rate of growth of MCF-7 cells (Figure 1). However, octreotide inhibited proliferation of MCF-7 cells at treatment times of more than three days. This was time- and dose-dependent — in the presence of octreotide at increasing concentrations (10 nM, 100 nM and 0.01 mM), a significant suppression of cell growth was observed on day 7; the cell number had decreased by $80 \pm 4.1\%$, $68 \pm 6.2\%$, and $51 \pm 2.1\%$, respectively, compared with the controls ($p < 0.001$). In agreement with previous findings [20–22], our results indicated that octreotide, synthesized in our laboratory, is responsible for this antiproliferative activity in MCF-7 cells.

In contrast to the study by Sharma and Srikant [23], who demonstrated that octreotide stimulates apoptosis in MCF-7 cells by inducing wide-type p53, a tumor suppressor protein, Bax and acidic endonuclease, octreotide synthesized in our laboratory did not induce apoptosis in MCF-7 cells (shown by observing the chromatin condensation by electron microscopy and the Hoechst 33258 nuclear stain [data not shown]). The difference in the findings could be due to the source of octreotide or to differential expression of SSTR subtypes in MCF-7 cells cultured in the different laboratories. In our laboratory, we analysed apoptosis in MCF-7 cells by directly observing cell ultrastructure using electron microscopy, rather than flow-cytometric measurement, which was used by Sharma and Srikant [23]. As stated earlier the different results might be explained further by determining SSTR subtypes expressed in MCF-7 cells cultured in our laboratory.

Figure 1

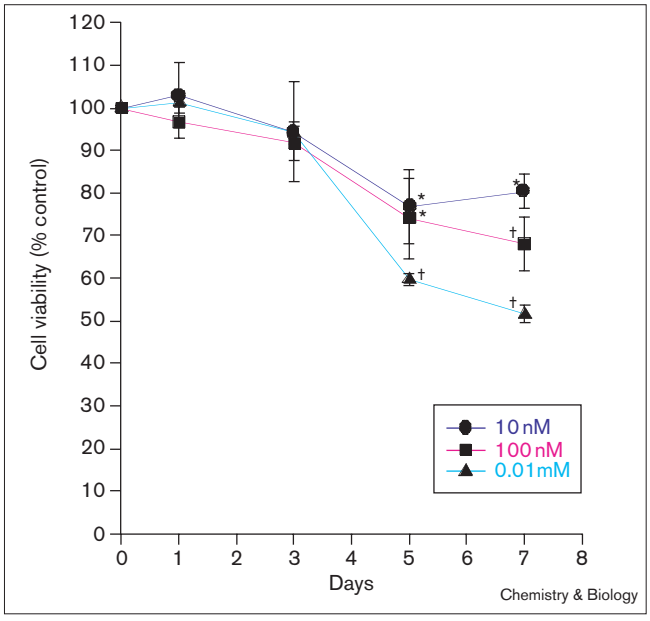

Effect of octreotide on cell growth. MCF-7 cells were treated with 10 nM (●), 100 nM (■) or 0.01 mM (▲) octreotide for seven days. Long-term (i.e. more than three days) treatment of octreotide exerts an inhibitory effect on cell growth. Data are mean ± SE (bars) values from three independent experiments. *p <0.01, †p <0.001, compared with control cells (without octreotide treatment at 0 day) using student's *t* test.

To this aim, the reverse transcription polymerase chain reaction (RT-PCR) will be performed in future studies, using primers for individual SSTRs.

Five distinct SSTRs have been cloned from humans, mice and rats and classified on the basis of their ability or inability to bind octapeptide SST analogs [24] into distinct subfamilies; one comprising SSTR-2, -3 and -5, the other SSTR-1 and -4. Cyclic hexapeptide and octapeptide SST analogs bind to the first group, (SSTR-2, -3 and -5), but not to SSTR-1 and -4. MCF-7 cells have been shown to express SSTR-1, -2, -4 and -5 but not SSTR-3 [25]. It is likely, therefore, that the antiproliferative action of octreotide is mediated through SSTR-2 or -5 or both. SST induces apoptosis uniquely through human SSTR-3 [26]. In Chinese hamster ovary K-1 (CHO-K1) cells, this SSTR-3-induced apoptosis is characterized by the appearance of oligonucleosomal DNA and is associated with the induction of wild-type (wt) p53 and Bax [26]. As MCF-7 cells do not express SSTR-3, however, the SSTR-3-mediated apoptotic effects of octreotide could not be expressed in these cells cultured in our laboratory.

Internalization of fluorescein-labeled octreotide in MCF-7 cells

Previously, radiolabeled octreotide was used for imaging SSTR-positive tumors through the binding of octreotide

Figure 2

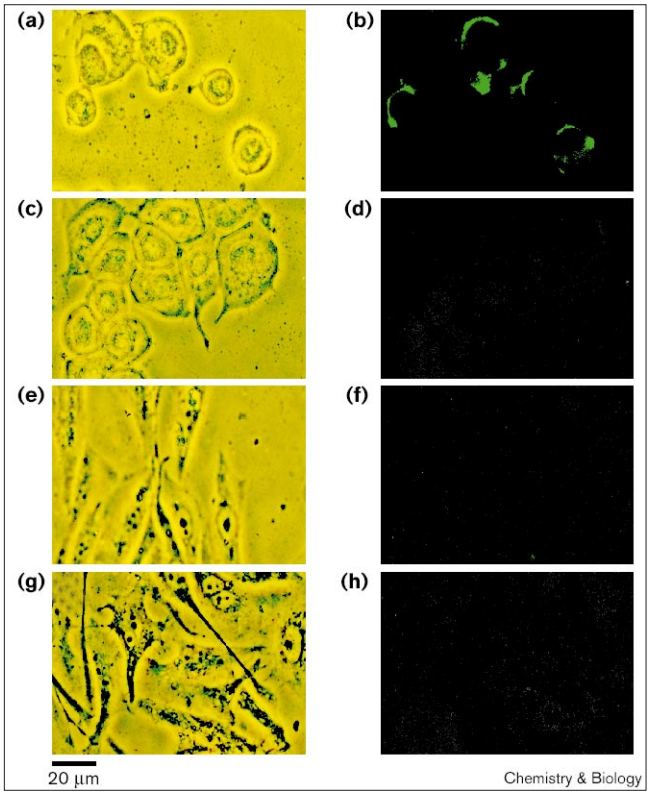

(b,d,f,h) Fluorescence micrographs of MCF-7 and CHO cells after incubation with 100 μg/ml fluorescein-labeled octreotide at 4°C for 30 min. (b) The labeling is confined to the MCF-7 cell surface. (d) The labeling is no longer apparent in MCF-7 cells incubated in the presence of an excess of nonfluorescent octreotide (100 mg/ml). (f) No labeling was seen in CHO cells, even in cells incubated with 500 μg/ml fluorescein-labeled octreotide (h). **(a,c,e,g)** Cell morphologies under the associated conditions.

Figure 3

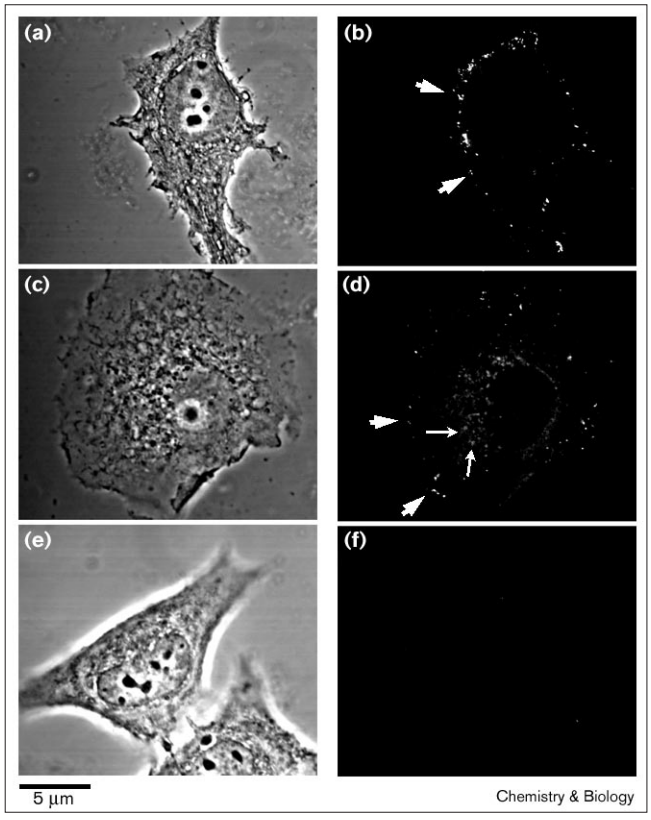

Confocal microscopic imaging of internalized fluorescein-labeled octreotide in MCF-7 cells. **(a,b)** After 10 min of incubation with 100 μg/ml fluorescein-labeled octreotide at 37°C, fluorescent labels are mainly apparent at periphery of the cell (arrowheads). **(c,d)** At 1 h, most label is clustered around the nucleus (arrows). **(e,f)** No fluorescence was seen in cells incubated with 100 mg/ml octreotide (without fluorescein tag) for 1 h prior to incubation with fluorescein-labeled octreotide for 10 min.

to an SSTR [27]. Fluorescein-labeled octreotide presents a relatively safe way to visualize the interaction between octreotide and an SSTR. We successfully synthesized fluorescein-labeled octreotide using p-carboxybenaldehyde as a linker by which to anchor fluoren-9-ylmethoxycarbonyl (Fmoc)-throneninol to solid-phase resins, and then fluorescein in the final coupling cycle.

Although octreotide is a peptide-based drug, it has remarkable stability in the presence of degradative enzymes (compared to native SST) [28]. It is expected that octreotide will not be degraded in incubation medium containing bovine fetal serum. Observations thereafter can ignore effects caused by octreotide degradation in medium. In agreement with this, high-performance liquid chromatography (HPLC) analysis demonstrated that octreotide and fluorescein-labeled octreotide were not degraded after 24 h of incubation in DMEM containing 1% bovine fetal serum (data not shown). In order to evaluate whether octreotide demonstrates specific targeting in SSTR- expressing cells, we analysed the binding of fluorescein-labeled octreotide in two cell lines: MCF-7 cells (presenting high-affinity binding sites for octreotide) and CHO cells (which express low levels of SSTR [196 fmol/mg protein]) [29]. Incubation of MCF-7 cells with fluorescein-labeled octreotide (100 μg/ml) at 4°C for 30 min resulted in a specific but diffusely distributed fluorescein along the cell surface of MCF-7 cells (Figures 2a,b), whereas upon incubation at 37°C for 10 min under parallel conditions, denser fluorescent grains were visible mainly at the cell periphery (Figure 3a,b). At 1 h (Figure 3c,d), fluorescent grains were distributed throughout the cytosol of the cell and many grains were clustered at the periphery of cell nucleus. These results suggest that this octreotide conjugate binds SSTR and then is internalized via SSTR-mediated endocytosis in MCF-7 cells. Fluorescence is no longer apparent in MCF-7 cells pretreated with 1000-fold excesses of unlabeled octreotide for 1 h at 4°C (Figure 2c,d) or 37°C (Figure 3e,f).

No labeling was seen in CHO cells when incubated with 100 μg/ml or 500 μg/ml of fluorescein-labeled octreotide (Figure 2f,h). These results indicate that octreotide is a powerful drug carrier to deliver the drugs into SSTR-expressing cells.

To develop novel, targeted antitumor agents for the treatment of various cancer-cell-expressing receptors for SST, we conjugated octreotide to taxol, a diterpenoid plant product, and demonstrated its superior antitumor activity by binding preferentially to the amino-terminal region of the β-tubulin subunit of microtubule polymers. Taxol is an effective drug that shows efficacy in human ovarian and metastatic breast cancers [30,31] and malignant melanoma [32]. The molecular mechanisms underlying taxol-induced apoptosis of MCF-7 cells have been studied. Such mechanisms studied include $p34^{cdc2}$ kinase activation [33], and $p21^{Waf1}$ and p53 induction [34]. The role of taxol in combating certain cancers and our current understanding of the underlying mechanisms make it a good candidate for an antitumor drug linked to octreotide. The cell specificity of the antitumor effect of taxol is low, so it is highly toxic in most human cells when a cancer patient is treated with taxol-based chemotherapy [16,17]. The design of taxol linked to a tumor tracer, such as octreotide, may be employed to enhance the cell specificity and selectivity of taxol.

Design and synthesis of octreotide-conjugated taxol

The design for synthesis octreotide-conjugated taxol was based on the properties of SSTR endocytosis when octreotide binds to SSTR. Octreotide-conjugated taxol internalization into the cytosol of SSTR-expressing tumor cells could decrease the cytotoxicity of taxol in non-SSTR-expressing cells. When designing such a conjugate, we sought to retain the binding properties of the carrier peptide, as well as the antitumor activity of taxol. First, fluorescein-labeled octreotide was synthesized in order to test its SSTR binding properties (described above). Structure–activity studies on taxol revealed that the C-13 ester sidechain and its 2′-hydroxl group appear essential for tubulin binding [35,36]. The observation therefore suggests that the 2′ and 7′ position are suitable sites for reversible derivatization [37,38]. The creation of taxol-conjugated octreotide is depicted in Figure 4. Taxol-succinate (2′-succinyl-paclitaxel) was synthesized by following the procedure described by Deutsch *et al.* [37], and was activated by benzotriazol-1-yloxy-tris-pyrrolidinophosphonium (PyBOP) in dimethyl formamide (DMF) before being coupled to the α amino group at the amino terminus of octreotide, which was bound to Siber amide resin. Octreotide (NH_2-D-Phe–c[Cys–Phe–D-Trp–Lys(Mtt)–Thr–Cys]–Thr-ol-acetal; Mtt, 4-methyltrityl), was synthesized to Siber amide resin using solid-phase Fmoc chemistry, followed by on-resin disulfide formation after oxidation by thallium(III)-trifluoroacetate in DMF at 0°C for 80 min [13,39].

It has been pointed out that the taxol molecule is fragile in strongly acidic conditions and no pure product could be isolated after a standard acidic cleavage and deprotection [37,38]. Siber amide resin, which has an acid-sensitive

Figure 4

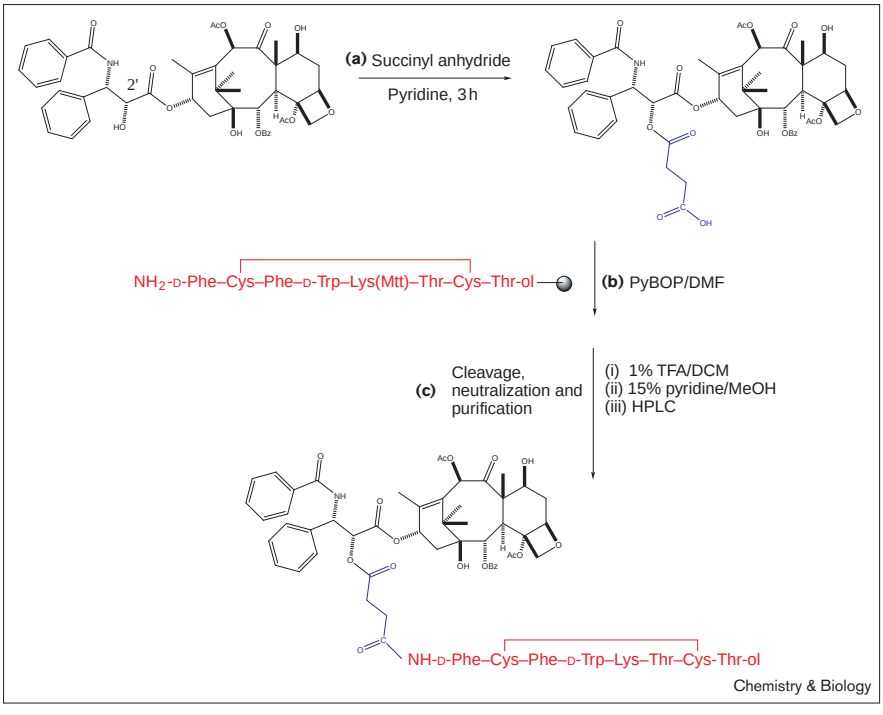

Molecular structure of octreotide-conjugated taxol. Paclitaxel succinate is conjugated to the amino terminus of octreotide. **(a)** Paclitaxel and succinic anhydride are dissolved in pyridine and stirred for 3 h. **(b)** Paclitaxel succinate is activated by PyBOP in DMF and reacted with the amino terminus of octreotide. **(c)** The peptide conjugate is deprotected and cleaved from the amide resin by addition of 1% TFA/DCM; compounds are neutralized using 15% pyrinidine in methanol before purification using HPLC.

Figure 5

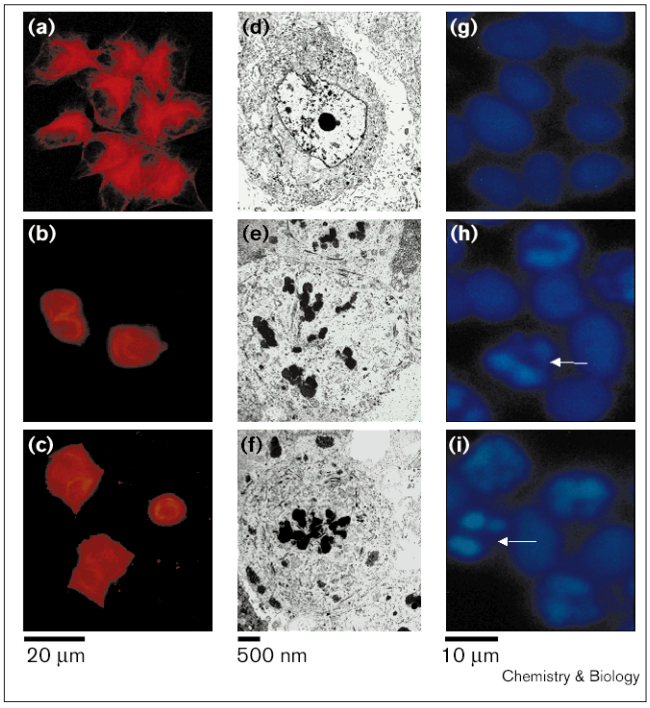

Octreotide-conjugated taxol virtually retains the cellular functions of taxol. **(a,b,c)** Distribution of β tubulin in MCF-7 cells. Cells were (a) in the absence of both taxol and octreotide-conjugated taxol (b) the presence of 10^{-6} M taxol or (c) octreotide-conjugated taxol. **(d–i)** Chromatin condensation in apoptotic cells. (d–f) Ultrastructure of apoptotic MCF-7 cells as observed using transmission electron micrography (×7500). (g–i) Nuclei were stained with Hoechst 33258 and fluorescence photomicrographs were taken. MCF-7 cells were treated without (d,g) or with 10^{-6} M taxol (e,h) or octreotide-conjugated taxol (f,i) for 24 h. Arrows indicate chromatin condensation in apoptotic cells.

Figure 6

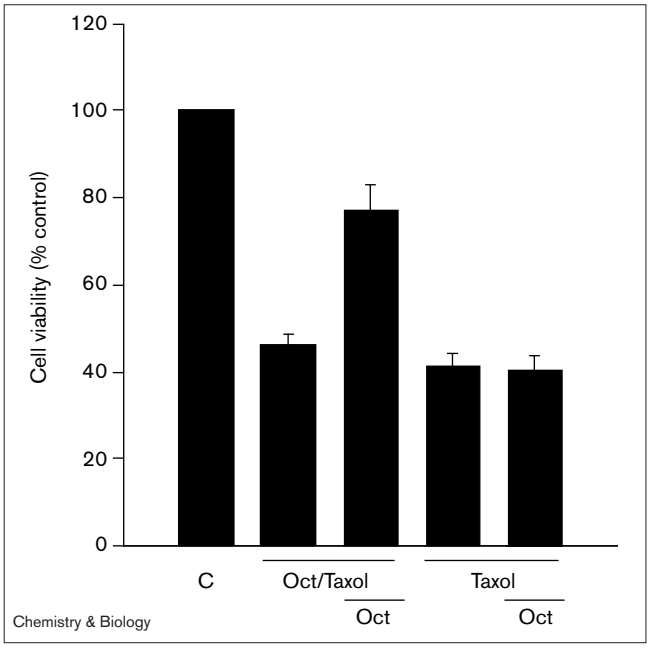

Pretreatment with octreotide antagonizes the cytotoxicity of octreotide-conjugated taxol, but treatment with taxol alone does not. MCF-7 cells were pretreated with 10^{-2} M octreotide (Oct) for 30 min prior to treatment with 10^{-5} M taxol, or octreotide-conjugated taxol (Oct/Taxol) for 24 h. Data are mean ± SE (bars) values from three separate measurements, using three different batches of cells.

linker, was therefore used as the solid support to avoid the strong acidic conditions of trifluoroacetic acid (TFA) cleavage and to prevent the taxol molecule from being damaged.

Biological properties of octreotide-conjugated taxol

To investigate whether octreotide-conjugated taxol retains the biological properties of taxol [40], we treated MCF-7 cells with 10^{-6} M taxol and with octreotide-conjugated taxol for 8 h. The change in microtubules was visualized by indirect immunofluorescent staining using β-tubulin antibody (Figure 5a–c). Cell morphology is thought to be maintained by the cytoskeleton; reorganization of the cytoskeletal networks was therefore explored using fluorescence microscopy. It was found that, after an 8 hour treatment with 10^{-6} M taxol or octreotide-conjugated taxol, MCF-7 cells showed extensive clustering of tubulin around nuclei (Figure 5b,c). Tubulin bundles were visualized in orange (intensive rhodamine staining) and quantified by counting over 800 cells. In the presence of taxol or octreotide-conjugated taxol (10^{-6}, 10^{-5} and 10^{-4} M), the percentages of cells containing tubulin bundles were 67%, 83% and 92%, respectively, for taxol treatment, and 65%, 81% and 93%, respectively, for octreotide-conjugated taxol treatment (data not shown). Octreotide-conjugated taxol and taxol were therefore equally active regarding microtubule bundle formation.

Understanding the properties of these two drugs with respect to induction of apoptosis was also of interest. We distinguished between viable and apoptotic cells on the basis of cellular nuclear chromatin pattern, which was assessed by fluorescent microscopic analysis of nuclei stained with Hoechst 33258 (Figure 5g–i), and by electron microscopy (Figure 5d–f). The nuclear chromatin of viable MCF-7 cells was dispersed, whereas that of apoptotic cells was condensed into densely fluorescent apoptotic nuclear fragments. We have found that both drugs can induce chromatin condensation after 24 h treatment (Figure 5e,f), and from observations using electron microscopy, we also have found that the nuclear membrane disappeared after treatment with both taxol and octreotide-conjugated taxol under these conditions. Both drugs induce $p34^{cdc2}$ kinase activation, which controls the G_2 to M phase transition by promoting breakdown of the nuclear membrane and chromatin condensation [29,33,41].

Figure 5 therefore illustrates clearly that octreotide-conjugated taxol retains the ability of taxol to bind β-tubulin subunits of microtubule polymers and to trigger apoptosis of MCF-7 cells.

To determine whether octreotide-conjugated taxol causes cytotoxicity via association with SSTRs, we pretreated MCF-7 cells with 10^{-2} M octreotide for 1 h prior to treatment of 10^{-5} M octreotide-conjugated taxol or taxol alone for 24 h (Figure 6). Treatment for 24 h with octreotide alone did not affect the cell viability significantly (see Figure 1). However, after treatment with 10^{-5} M octreotide-conjugated taxol or free taxol for 24 h, cell viability was 46 ± 2.7% and 41 ± 3.3% compared with controls. Pretreatment with 10^{-2} M octreotide resulted in a significant increase in viability (77 ± 6.2%) of MCF-7 cells that are treated with octreotide-conjugated taxol for 24 h. Pretreatment of octreotide therefore antagonizes the cytotoxicity of octreotide-conjugated taxol. However, pretreatment of octreotide cannot antagonize the cytotoxicity of taxol. Owing to the hydrophobic nature of taxol, it has been suggested that taxol is transported across membranes by passive diffusion [42]. Our results show that, unlike free taxol, octreotide-conjugated taxol causes cytotoxicity mainly mediated by the endocytosis of SSTR. Octreotide-conjugated taxol, performed by coupling succinylated taxol to the amino terminus of octreotide, seems not to be degraded until it is internalized into the cytosol of MCF-7 cells.

Cell-specific differences in cytotoxicity of octreotide-conjugated taxol

Antiproliferative activities of taxol and octreotide-conjugated taxol were evaluated in MCF-7 and CHO cells. Drug concentrations that inhibited cell growth by 50% are presented as IC_{50} values, and taxol had IC_{50} values of 10^{-7} and 10^{-6} M in MCF-7 and CHO cells, respectively

Figure 7

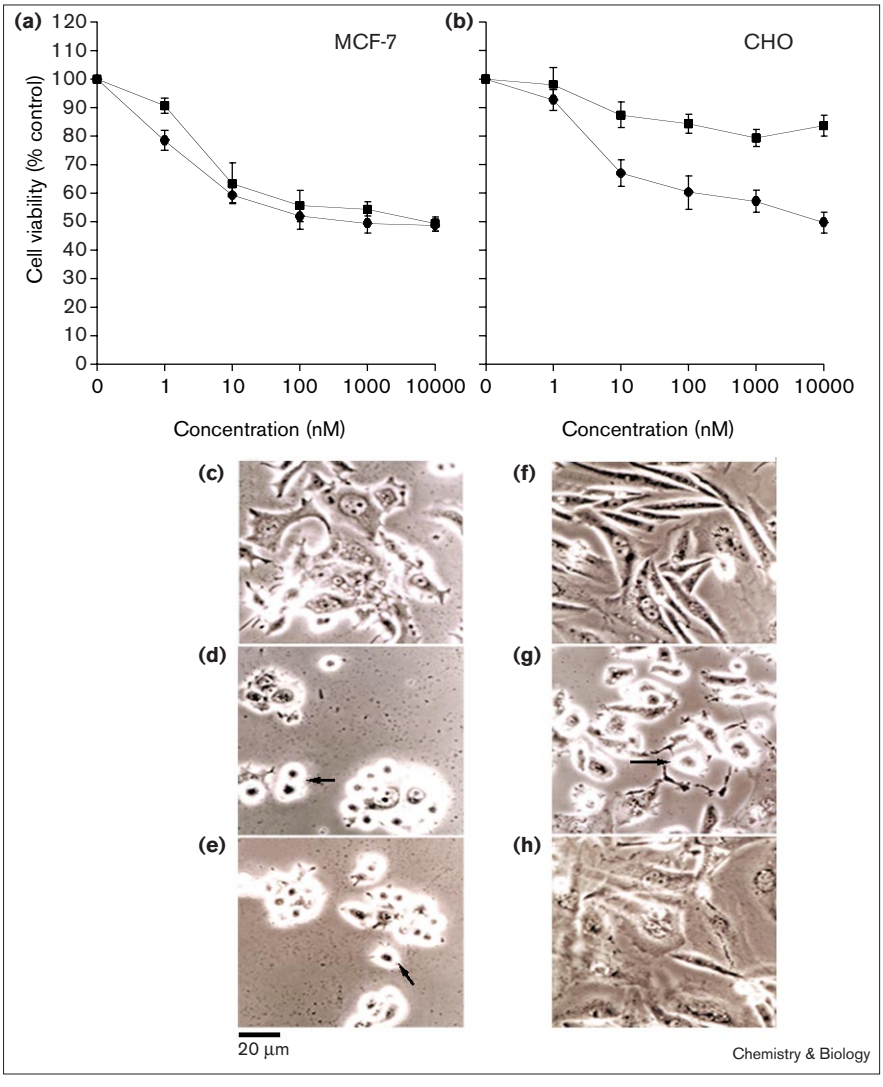

Cell specificity of octreotide-conjugated taxol. **(a)** Like free taxol (●), octreotide-conjugated taxol (■) induced dose-dependent cell death in MCF-7 cells at 1, 10, 100, 1000 and 10,000 nM. Data of treatments with higher concentrations were not shown due to precipitation in cell media. **(b)** Unlike free taxol, octreotide-conjugated taxol is significantly less toxic in CHO cells. MCF-7 **(c–e)** and CHO **(f–h)** cells were treated with 10^{-5} M taxol (d,g) or octreotide-conjugated taxol (e,h) for 24 h. Cell death was indicated by arrows. Data are mean ± SE (bars) values of five separated measurements, using five different batches of cells experiments.

Figure 8

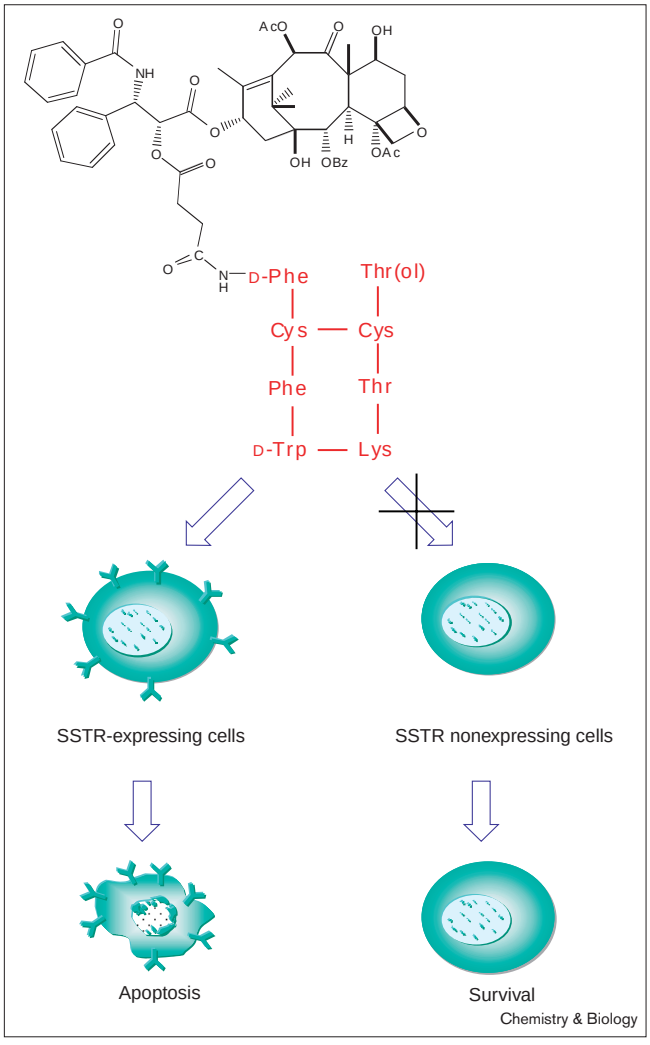

The octreotide-conjugated taxol serves as a targeted antitumor drug for treatment of various tumors expressing SSTRs. Octreotide-conjugated taxol causes cytotoxicity mainly mediated by the endocytosis of SSTR. It induces cell death exclusively in cells expressing high levels of SSTRs. Bz, benzoyl; Ac, acetyl.

(Figure 7). Both drugs caused precipitates in cell media at concentrations higher than 10^{-5} M, and cell growth remained at the same lowest level; thus Figure 7 does not show the results of treatments at higher concentrations.

In agreement with earlier findings [42], species-specific differences in taxol cytotoxicity against human and rodent tumor cells could result from the presence of different taxol transport systems. The octreotide-conjugated taxol, which is slightly less toxic than taxol, induced dose-dependent cell death in MCF-7 cells. Unlike taxol alone, the cytotoxicity of octreotide-conjugated taxol is much lower in CHO cells. These results suggest that cells that express low levels of SSTRs (e.g. CHO cells) are highly resistant to octreotide-conjugated taxol. Moreover, octreotide-conjugated taxol induces cell death in a cell-specific manner — that is, exclusively in cells expressing high levels of SSTRs.

Significance

Most cytotoxic antitumor drugs suffer from a common problem: toxic side effects due to a lack of drug selectivity. The antiproliferative effects of chemotherapeutic agents such as mitomycin C, doxorubicin, 5-fluorouracil and taxol are synergistically enhanced by co-treatment with octreotide *in vitro* and *in vivo* [43]. However, when doxorubicin or its superactive derivative, 2-pyrrolino-doxorubicin, are linked chemically to the analogs of somatostatin (SST), octapeptides RC-160 and RC-121 [44], the cytotoxicity of doxorubicin or 2-pyrrolinodoxorubicin is decreased or maintained at the same level in various tumor cell lines. Therefore, using endocytotic ligands as carriers of the anticancer drugs to target these drugs to the cancer cells, these toxic side effects can be dramatically decreased and the efficacy of these drugs greatly improved. In previous studies [45], octreotide proved to be more potent in inhibiting the secretion of growth hormone and to have a longer plasma half life than native SST. Therefore, it is a particularly desirable peptide for development as a targeted antitumor drug. Moreover, the high-level expression of SSTRs on various tumor cells compared with normal tissue or blood affords its successful use as a tumor tracer. Octreotide D-Phe–c[Cys–Phe–D-Trp–Lys–Thr–Cys]–Thr-[ol] labeled with fluorescein is a powerful tool to visualize tumors that express SST receptors and can be predictive in determining whether a patient should receive SST octapeptide hormone therapy.

Octreotide-conjugated taxol retains taxol's ability to induce apoptosis (Figure 8) via binding the β-tubulin subunit of microtubule polymers. Octreotide-conjugated taxol, but not free taxol, is toxic exclusively to tumor cells expressing SSTRs. Therefore, it may prove highly valuable to develop octreotide-conjugated antitumor drugs.

Materials and methods

Materials

Fmoc amino acids, Rink AM resin, Siber amide resin and PyBOP were purchased from Novobiochem (San Diego, CA). Fmoc-Thr-(ol)-benzo-acetal was prepared previously in our laboratory [13]. Triisopropylsilane (TIS) was purchased from Acros, NJ. MCF-7 cells were obtained from the American Type Culture Collection (Rockville, MD). DMEM, fetal bovine serum, L-glutamine, penicillin (19 000 units), streptomycin (10 mg/ml) and trypsin, EDTA (10×; 0.5% trypsin–5.3 mM EDTA) were purchased from Gibco BRL Life Technologies (Grand Island, NY). Taxol was obtained from Hauser Inc. (Boulder, CO, USA). Taxol was dissolved in 95% ethanol before being diluted into incubation medium immediately before experiments. Bisbenzimide trihydrochloroacetic acid (Hoechst 33258,) and MTT (3-[4,5-dimethylthiazol-2,5]-diphenyl tetrasolium bromide) were

obtained from Sigma Chemical Co. (St. Louis, MO). All other chemicals were obtained from Merck (Darmstadt, Germany).

Cell culture

MCF-7 breast tumor cells were maintained in DMEM supplemented with glutamine (0.292 mg/ml), penicillin/streptomycin (0.5 ml/100ml medium), 1% bovine fetal serum at 37°C under 5% CO_2. The medium was changed every two to three days. To assay of cell survival, the viability was measured used trypan blue exclusion and MTT assay kit [46].

Synthesis of fluorescein-β-alanine-octreotide

Four equivalent of 5(6)-carboxy-fluorescein (0.4 mmole) were coupled to the amino terminus of the assembly chain of NH_2-β-Ala-D-Phe–c[Cys–Phe–D-Trp–Lys(Mtt)–Thr–Cys]–Thr-ol-acetal-amide resin (0.1 mmol) [13]. The coupling reaction was conducted in an aluminum-foil-wrapped vessel. Direct light exposure was avoided thereafter. Cleavage of the peptide conjugate from the amide resin was achieved using 95% TFA/5% TIS. After evaporation of TFA under vacuum, the residue was washed and precipitated by addition of ice-cold dry ether. The precipitate was filtered on a sintered glass funnel and extracted using 20% acetic acid solution. After lyophilization, the product was loaded onto a Vydac C18 preparative column (Hesperia, CA) and purified. Electrospray ionization mass spectrometry (ESI–MS) result gave $[M+H]^+$ mass/charge (m/z) value of 1448 Da.

Synthesis of paclitaxel succinate

Paclitaxel succinate was synthesized by following the procedure described by Deutsch *et al.* [37]. Paclitaxel (0.43 g, 0.5 mmol) and succinic anhydride (0.6 g, 6 mmol) were dissolved in 10 ml of pyridine and stirred at room temperature for 3 h. At the end of the reaction, the solution was evaporated to dryness *in vacuo*. The residue was treated with 20 ml ice-cold water, stirring for 20 min, and filtered. The precipitate was redissolved in acetone and then water was added to produce fine crystals of paclitaxel succinate (0.42 g with an 86% yield). ESI–MS gave $[M+H]^+$ m/z 954 Da

Synthesis of paclitaxel-succinyl–octreotide

The expected compound and synthetic procedure is illustrated in Figure 4. Four equivalents of paclitaxel succinate activated by PyBOP in DMF were added to resin-bound octreotide (0.1 mM) [39]. The end of the reaction (i.e. binding of pacilitaxel succinate to the amino terminus of octreotide) was monitored by the ninhydrine test, which measured loss of the free amino group at amino terminus of lysine-protected octreotide. Cleavage and sidechain deprotection of the peptide conjugate from the amide resin was achieved using 1% TFA/5% TIS/dichloromethane (DCM). Compounds were neutralized using 15% pyridine/methanol. The sample was lyophilized to 135 mg crude product (69% crude yields). HPLC analysis was performed with a Vydac C18 column (10 × 250 mm) with the eluent system: 30% B in A (A: 5% acetonitrile (ACN)/95% H_2O/0.1% TFA; B: 95% ACN /5% H_2O/0.1% TFA) to 90% B with a linear gradient for 30 min. The compound with a retention time of 10.1 min (~34% purity calculated from the peak area) was isolated and analysed to give $[M+H]^+$ values of 1954 Da using ESI–MS.

Morphological determination of levels of apoptosis

Morphological determination of levels of apoptosis was preformed by labeling the cells with the nuclear strain Hoechst 33258 and visualization by fluorescence microscopy [47]. Transmission electron microscopy was also used to observe apoptotic cells [48]. Cells were fixed in cold 4% glutaraldehyde in 0.1 M cacodylate buffer (pH 7.4) at 4°C, dehydrated in grade acetone, passed through propylene oxide, and embedded in EMbed-812 (Purchased from EMS, Fort Washington, PA). Ultra-thin sections were cut and stained with uranyl acetate and alkaline bismuth subnitrate and viewed under a Siemens Elmiskop 102 electron microscope at 80 kV.

Fluorescence microscopy for β tubulin

Coverslips were coating with fetal bovine serum at 37°C for 30 min. Cultured MCF-7 cells on coverslips were fixed by 2% formaldehyde. Fixed cells were washed with Dulbecco's phosphate buffered saline (PBS) for 5 min at room temperature and then permeabilized by acetone at −20°C for 3 min. The permeabilized cells were then stained with anti-β-tubulin antibody (1:200) in the presence of 1% (w/v) bovine serum albumin (BSA) for 1 h. Cells were washed twice, for 10 min each time, with PBS and then incubated with rhodamine-conjugated goat antimouse immunoglobulin (1:200) for 1 h. The stained cells were mounted in 50% (v/v) glycerol in PBS for observation by fluorescence microscope.

Confocal microscopy

Cells were incubated with fluorescein-labeled octreotide in PBS buffer containing 2 mM $MgCl_2$ and 0.1 % BSA. Labeled cells were examined under a Zeiss LSM 310 microscope configured with a Axioplan equipped with an argon laser.

Acknowledgements

We appreciate L-C Tsai for his helpful suggestions and comments. We thank S-F Yeh for her helpful instruction in β-tubulin immunofluorescent staining. S-P Lee's help in confocal analysis is highly appreciated. This study was supported by grants from the National Science Council (NSC 1234-5678) and Academia Sinica, Taipei, Taiwan.

References

1. Reichlin, S. (1983). Somatostatin. *New Engl. J. Med.* **309**, 1495-1501, 1556-1563.
2. Schally, A.V. (1988). Oncological applications of somatostatin analogs. *Cancer Res.* **48**, 6977-6985.
3. Lamberts, S.W.J., Krenning, E.P. & Reubi, J.C. (1991). The role of somatostatin and its analogs in the diagnosis and treatment of tumors. *Endocr. Rev.* **12**, 450-482.
4. Goldstein, J.L., Brow, M.S., Anderson, R.G., Russell, D.W. & Schneider, W.J. (1985). Receptor-mediated endocytosis: concepts emerging from the LDL receptor system. *Annu. Rev. Cell Biol.* **1**, 1-39.
5. Bauer, W., *et al.*, & Pless, J. (1982). SMS 201-995: a very potent and selective octapeptide analogue of somatostatin with prolonged action. *Life Sci.* **31**, 1133-1140.
6. Virgolini, I., *et al.*, & Dean, R. (1998). Somatostatin receptor subtype specificity and *in vivo* binding of a novel tumor tracer, ^{99m}Tc-P829. *Cancer Res.* **58**, 1850-1859.
7. Reubi, J.C., Lang, W., Maurer, R., Koper, J.W. & Lambert, S.W.J. (1987). Distribution and biochemical characterization of somatostatin receptors in tumors of the human central nervous system. *Cancer Res.* **47**, 4758-4764.
8. Hoelting, T., Duh, Q., Clark, O.H. & Herfarth, C. (1996). Somatostatin analog octreotide inhibits the growth of differentiated thyroid cancer cells *in vitro*, but not *in vivo*. *J. Clin. Endocrinol.* **15**, 2638-2641.
9. Raynor, K., *et al.*, & Reisine, T. (1993). Characterization of cloned somatostatin receptors SSTR4 and SSTR5. *Am. Soc. Pharmacol. Exp. Ther.* **16**, 385-392.
10. Simpkins, H. & Parekh, H. (1996). Species-specific differences in taxol transport and cytotoxicity against human and rodent tumor cells. *Biochem. Pharmacol.* **51**, 301-311.
11. Lambert, S.W.J., Krenning, E.P. & Rebui, J.-C. (1991). The role of somatostatin and its analogs in the diagnosis and treatment of tumors. *Endocr. Rev.* **12**, 450-482.
12. Bakker, W.H., Kreening, E.P. & Breeman, W.A.P. (1991). *In vivo* use of a radiolabelled somatostatin analog: dynamics. Metabolism and binding to somatostatin receptor-postive tumors in man. *J. Nucl. Med.* **33**, 652-658.
13. Wu, Y.-T., *et al.*, & Wang, K.-T. (1998). Facile solid phase synthesis of octreotide analogs p-carboxybenzaldehyde as a linker to anchor Fmoc-threninol to solid phase resins. *Tetrahedron Lett.* **39**, 1783-1784.
14. Rowinsky, E.K., Onetto, N., Canetta ,R.M. & Arbuck, S.G. (1992). Taxol: The first of the taxanes, an important new class of antitumor agents. *Semin. Oncol.* **19**, 646-662.
15. Rowinsky , E.K. & Donehower, R.C. (1993). The clinical pharmacology of paclitaxel (taxol). *Semin. Oncol.* **20**, 16-25.
16. Liebmann , J.E., *et al.*, & Mitchell, J.B. (1993). Cytotoxic studies of paclitaxel (taxol) in human tumor cell lines. *Br. J. Cancer* **68**, 1104-1109.
17. Wani, M.C., Taylor, H.L., Wall, M.E., Coggon, P. & NcPhail, A.T. (1971). Plant antitumor agents VI. The isolation and structure of taxol,

a novel antileukemic and antitumor agent from *Taxus brevifolia*. *J. Am. Chem. Soc.* **93**, 2325-2327.
18. Chu, J.-J., *et al*., & Lai, .Y.-K. (1998). Taxol induces concomitant hyperphosphorylation and reorganization of vimentin intermediate filaments in 9L rat brain tumor cells. *J. Cell. Biochem.* **68**, 472-483.
19. Horwitz, S.B. (1992). Mechanism of action of taxol. *Trends Pharmacol. Sci.* **13**, 134-136.
20. Hofland, L.J., *et al*., & Lamberts, S.W.J. (1992). Dissociation of antiproliferative and antihormonal effects of the somatostatin analog octreotide on 7315b pituitary tumor cells. *Endocrinology* **131**, 571-577.
21. Hofland, L.J., *et. al*., & Lamberts, W.J. (1995). Role of tumor-derived fibroblasts in the growth of primary cultures of human breast-cancer cells: effects of epidermal growth factor and the somatostatin analogue octreotide. *Int. J. Cancer* **60**, 93-99.
22. Setyono-Han, B., Henkelman, M.S., Foekens, J.A. & Klijn, J G.M. (1987). Direct inhibitory effects of somatostatin (analogs) on the growth of human breast cancer cells. *Cancer Res.* **47**, 1566-1570.
23. Sharma, K. & Srikant, C.B. (1998). Induction of wild-type p53, BAX, and acidic endonuclease during somatostatin-signaled apoptosis in MCF-7 human breast cancer cells. *Int. J. Cancer* **76**, 259-266.
24. O'carroll, A.-M., Raynor, K., Lolait, S.J. & Reisine, T. (1994). Characterization of cloned human somatostatin receptor SSTR5. *Mol. Pharmacol.* **46**, 291-298.
25. Gregorakis, S.I., Robertson, L-A., Watson, P.& Patel, Y.C. (1995). MRNA expression of five human somatostatin receptor subtypes (hSSTR1-5) in human breast tumor tissues. *International Congress on Somatostatin Analogs: Basic and Clinical Perspectives, Sorrento, Italy*. Abstract 9.
26. Sharma, K.S., Patel, Y.C. & Srikant, C.B. (1996). Subtype-selective induction of wild-type p53 and apoptosis, but not cell cycle arrest, by human somatostatin receptor 3. *Mol. Endocrinol.* **10**, 1688-1696.
27. Hofland, L.J., *et al*., & Lamberts, S.W.J. (1995). Internalization of the radioiodinated somatostatin analog [^{125}I-Tyr^{3}]octreotide by mouse and human pituitary tumor cells: increase by unlabeled octreotide. *Endocrinology* **136**, 3698-3706.
28. Bauer, W., *et al*., & Pless, J. (1982). SMS 201-995: a very potent and selective octapeptide analogue of somatostatin with prolonged action. *Life Sci.* **31**, 1133-1140.
29. Manfredi, J.J., Parness, J., & Horwitz, S.B. (1982). Taxol binds to cellular microtubules. *J. Cell Biol.* **94**, 688-696.
30. Seidman, A.D., *et al*., & Norton, L. (1997). Paclitaxel for breast cancer: the memorial Sloan-Kettering cancer center experience. *Oncology* **11 (3 suppl 2)**, 20-28.
31. Dunton, C.J. (1997). New options for the treatment of advanced ovarian cancer. *Semin. Oncol.* **24 (1 suppl 5)**, S5-S2S511.
32. Holmes, F.A., *et al*., & Hortobagyi, G.N. (1991). Phase II study of taxol, an active drug in the treatment of metastatic breast cancer. *J. Natl. Cancer Inst.* **83**, 1797-1805.
33. Donaldson, K.L., Goolsby, G., Kiener, P.A. & Wahl, A.F. (1994). Activation of p34^{cdc2} coincident with taxol-induced apoptosis. *Cell Growth Differ.* **5**, 1041-1050.
34. Blagosklonny, M.V., *et al*., & Neckers L. (1995). Taxol induction of p21^{WAF1} and p53 requires c-raf-1. *Cancer Res. 55*, 4623-4626.
35. Wain, M.C., Taylor, H.L., Wall, M.E., Coogan, P.C. & McPail, A.J. (1971). Plant antitumor agents, IV. The isolation and structure of taxol, a novel antileukemic and antitumor agent from *Taxus brevifolia*. *J. Am. Chem. Soc.* **93**, 2325-2327.
36. Nicolaou, K.C., Dai, W.-M. & Guy, R.K. (1994). Chemistry and biology of taxol. *Angew. Chem. Int. Ed. Engl.* **33**, 15-44.
37. Deutsch, H.M., *et al*., & Zalkow, L.H. (1989). Synthesis of congeners and prodrugs. 3. Water-soluble prodrugs of taxol with potent antitumor activity. *J. Med. Chem.* **32**, 788-792.
38. Mathew, A.E., Mejillano, M.R., Nath, J.P., Himes, R.H. & Stella, V.J. (1992). Synthesis and evaluation of some water-soluble prodrugs and derivatives of taxol with antitumor activity. *J. Med. Chem.* **35**, 145-151.
39. Wu, Y.-T., Hsieh, H.-P., Chen, S.-T. & Wang, K.-T. (1999). Direct solid phase synthesis of biologically active peptide alcohols. *J. Chin. Chem. Soc.* **46**, 135-138.
40. Bollag, D.M., *et al*., & Woods, C.M. (1995). Epothilones, a new class of microtubule-stabilizing agents with a taxol-like mechanism of action. *Cancer Res.* **55**, 2325-2333.
41. Djabali, K. (1999). Cytoskeletal proteins connecting intermediate filaments to cytoplasmic and nuclear preipery. *Histol. Histopathol.* **14**, 501-509.
42. Parekh, H. & Simpkins, H. (1996). Species-specific differences in taxol transport and cytotoxicity against human and rodent tumor cells. *Biochem. Pharmacol.* **51**, 301-311.
43. Weckbecker, G., Raulf, F., Tolcsvai, L. & Bruns, C. (1996). Potentiation of the anti-proliferative effects of anti-cancer drugs by octreotide *in vitro* and *in vivo*. *Digestion* **57 (suppl 1)**, 22-28.
44. Nagy, A., *et al*., & Kahan, Z. (1998). Synthesis and biological evalution of cytotoxic analogs of somatostatin containing doxorubicin or its intensely potent derivative, 2-pyrrolinodoxorubicin. *Proc. Natl Acad. Sci. USA* **95**, 1794-1799.
45. Bayer, W., Briner, U. & Doephner, W. (1982). SMS 201-995: a very potent and selective octapeptide analogue of somatostatin with prolonged action. *Life Sci.* **31**, 1133-1140.
46. Plumb, J.A., Milroy, R. & Kaye, S.B. (1989). Effect of the pH dependence of 3-(4,5-dimethylthiazol-2-yl)-2,5-diphenyl-tetrazolium bromide-formazan absorption on chemosensitivity determined by a novel tetrazolium-based assay. *Cancer Res.* **49**, 4435-4440.
47. Hartfield, P.J., Mayne, G.C. & Murray, A.W. (1997). Ceramide induces apoptosis in PC12 cells. *FEBS Lett.* **401**, 148-152.
48. Hill, S.M. & Blask, D.E. (1988). Effects of the pineal hormone melatonin on the proliferation and morphological characteristics of human breast cancer cells (MCF-7) in culture. *Cancer Res.* **48**, 6121-6126.